Supporting Online Material for

SLAM is a microbial sensor, which regulates bacterial phagosome functions in macrophages.

Scott B. Berger[1,†,‡], Xavier Romero[1,†], Chunyan Ma[1], Guoxing Wang[1], William A. Faubion[1,2], Gongxian Liao[1], Ewoud Compeer[1], Marton Keszei[1], Lucia Rameh[5], Ninghai Wang[1], Marianne Boes[4], Jose R. Regueiro[1,3], Hans Christian Reinecker[6] and Cox Terhorst [1,‡]

[1] Division of Immunology, Beth Israel Deaconess Medical Center, Harvard Medical School, Boston, MA 02115

[2] Department of Internal Medicine, Mayo Clinic, Rochester, MN 55905

[3] Inmunologia, Facultad de Medicina, Universidad Complutense, Madrid, Spain

[4] Department of Dermatology, Brigham and Women's Hospital, Harvard Medical School, Boston, MA 02115

[5] Boston Biomedical Research Institute, Watertown, MA 02472

[6] Department of Gastroenterology, Massachusetts General Hospital, Harvard Medical School, MA 02114

[†] These authors contributed equally to this work.

[‡] To whom correspondence should be addressed. E-mail: terhorst@bidmc.harvard.edu and sberger@bidmc.harvard.edu

Nature Immunology: doi:10.1038/ni.1931

This PDF file includes:

Supplementary Figures S1 to S14.

SUPPLEMENTAL FIGURES

Supplementary Figure S1.

Absence of a major developmental defect in *Slamf1*$^{-/-}$ macrophages.

Peritoneal macrophages from *Slamf1*$^{-/-}$ and *Slamf1*$^{+/+}$ BALB/c mice were analyzed by flow cytometry to evaluate key cell surface markers expressed on F4/80+ macrophages. Cell surface marker staining (solid line) and unstained cells (dotted line) are shown.

Supplementary Figure S2.

Defective killing of *E. coli F18* by *Slamf1*$^{-/-}$ B6 primary peritoneal macrophages.

Peritoneal macrophages from *Slamf1*$^{+/+}$ (black bars) and *Slamf1*$^{-/-}$ B6 (white bars) mice were exposed to *E. coli* F18 for 1 hour and 100 μg/ml gentamicin for an additional hour, followed by 10 μg/ml gentamicin for the duration of the assay. Viable intracellular bacteria were quantitated by gentle lysis of the macrophages and subsequent plating on LB agar.

The result is representative of 2 independent experiments.

CFU = colony forming units

Supplementary Figure S3.

The *Slamf1*$^{-/-}$ B6 mice contain the 129 locus, as judged by cytofluorometric analyses of thymocytes and NK cells with haplotype specific antibodies directed against CD229 (129) and CD244 (B6).

Top panel: Thymocytes were stained with anti-CD229 (Ly9.1) mAb, which only recognizes the SLAM-family haplotype II (*e.g.*129) CD229 receptor.

Bottom panel: NK1.1 positive splenocytes were stained with anti-CD244 (CD244.2), which only recognizes the SLAM-family haplotype I *(e.g.* B6) CD244 receptor.

Flow cytometry histograms with specific antibody are in Red and isotype control in Black.

Slamf1$^{+/+}$ B6 (left panels) or *Slamf1*$^{-/-}$ (right panels) {B6x129} n=10 mice were used.

Supplementary Figure S4.

Both *Slamf1*$^{-/-}$ {129 x B6} and *Slamf1*$^{-/-}$ {129 x BALB/c} mice contain the 129 (SLAM - Family Haplotype II) derived SLAM-Family locus, as judged by RFLP.

Analysis of restriction fragment length polymorphism (RFLP) was performed by PCR using genomic DNA from *Slamf1*$^{-/-}$ {129 x B6}, *Slamf1*$^{-/-}$ {129 x BALB/c}, B6 and F1 (B6 x 129) mice. PCR of a short genomic region, which contains a SNP (NCBI number: Rs31532197) located downstream of the Ly108 (*Slamf6*) gene was performed. The restriction enzyme BssHII was used for digestion of the PCR product.

Supplementary Figure S5.

Defective Nox2 activity by *Slamf1*$^{-/-}$ B6 primary macrophages in response to *E.coli* F18.

Peritoneal macrophages from *Slamf1*$^{+/+}$ (filled circles) and *Slamf1*$^{-/-}$ B6 mice (open circles) were stimulated with *E. coli* F18 and superoxide production was measured with lucigenin on a luminometer. The data are expressed as percent increase over time 0. The result is representative of 2 independent experiments.

Supplementary Figure S6.

Increased Nox2 activity upon phagocytosis of *E.coli* F18 by SLAM-transfected RAW 264.7 macrophages.

SLAM-negative RAW 264.7 cells were transfected with mock (red squares) or SLAM (black circles) cDNA. Cells were allowed to phagocytose *E. coli* F18 or stimulated with PMA for the indicated times. Superoxide production was measured with lucigenin on a luminometer. The data are expressed as percent increase over time 0. The result is representative of 4 independent experiments.

Supplementary Figure S7.

Transferrin-endocytosis is not altered in *Slamf1*–/– primary macrophages.

Peritoneal macrophages from *Slamf1*$^{+/+}$ (black bars) and *Slamf1*$^{-/-}$ (white bars) B6 mice were incubated with transferrin-488 for the indicated time-points. Surface bound transferring-Alexa 488 was removed using a mild acid wash. Cells were then subjected to fluorescence microscopy where the total integrated intensity of the cell was calculated. A minimum of 50 cells were quantified for each time-point. The result is representative of 2 independent experiments.

Supplementary Figure S8.

Low density lipoprotein (LDL) endocytosis is not altered in *Slamf1*–/– primary macrophages.

Peritoneal macrophages from *Slamf1*$^{+/+}$ (black bars) and *Slamf1*$^{-/-}$ (white bars) B6 mice were incubated with Dil-Low Density Lipoprotein (Dil-LDL) for the indicated time-points. Surface bound LDL was removed using a mild acid wash. Cells were then subjected to fluorescence microscopy where the total integrated intensity of the cell was calculated. A minimum of 50 cells were quantified for each time-point. The result is representative of 2 independent experiments.

Supplementary Figure S9.

Delayed recruitment of Rab5 to crude extract-bead phagosomes of primary peritoneal macrophages isolated from *Slamf1*$^{-/-}$ BALB/c mice.

Peritoneal macrophages from *Slamf1*$^{+/+}$ and *Slamf1*$^{-/-}$ BALB/c mice were incubated with 3 μm beads coated with a crude preparation of *E. coli* outer membrane extracts at a 1:10 (cells: beads) ratio and fixed after 15, 30, 60 and 120 minutes. Cells were stained with anti-Rab5 followed by Alexa 488 secondary antibody. The graph shows quantification of phagosomal Rab5 integrated intensity at the indicated time points for *Slamf1*$^{+/+}$ (black bars) or *Slamf1*$^{-/-}$ (white bars) mice. A minimum of 50 beads were quantified for each time-point. The result is representative of 2 independent experiments.

Supplementary Figure S10.

Western blot of ΔIgV-CD3ζ SLAM.

Cells were transfected with a fusion protein comprised of the human SLAM ecto-domain (or a mutant lacking the IgV domain) and the human CD3ζ intracellular region. Cells were lysed, run on an SDS page and blotted for CD3ζ.

Supplementary Figure S11.

SLAM recognizes various strains of *E.coli*.

Jurkat cells were co-transfected with a fusion protein composed of the human SLAM ecto-domain and the human CD3ζ intracellular region, a luciferase reporter under the control of the IL-2 promoter, and the renellin-luciferase reporter. 10^7 *S. aureus* DU5873 (Blue), *E.coli* F18 (Red), MG1655 (purple), CAT4010 (Green), JM101 (Light Blue) or K12 (Orange), as shown on the X-axis, were added to 3 x 10^6 transfected cells. The results are representative of 5 independent experiments.

CAT4010 – MG1655 lacking Iron transporter protein.

Supplementary Figure S12.

High degree of homology between the loop regions of OmpC and OmpF from *E. coli* and *S. typhimurium*.

The boundaries of the extracellular loops are taken from Basle et al.[1] Amino acid residues in red indicate identical amino acids in OmpC and OmpF. Blue amino acid residues indicate conserved mutations. Bold amino acids indicate identical residues between *E.coli* and *S.typhimurium* OmpC or OmpF.

Supplementary Figure S13.

***Slamf1*-/- macrophages have no defect in Nox2 activity in response to an OmpC and OmpF double deficient *E. coli* mutant.**

Peritoneal macrophages from *Slamf1*$^{+/+}$ (filled circles) and *Slamf1*$^{-/-}$ B6 mice (open circles) were stimulated with a wt *E. coli* JM101 (top panel) or an OmpC and OmpF double deficient *E. coli* mutant HN705 (bottom panel) and superoxide production was measured with lucigenin on a luminometer. The data are expressed as percent increase over time 0. The result is representative of 2 independent experiments.

Supplementary Figure S14.

Figure S14. Model showing regulation of Gram-negative bacterial killing by SLAM.

SLAM enters the Gram-negative phagosome where it is involved in the recruitment of Vps34-15-Beclin to the early phagosome and the subsequent production of PI(3)P. PI(3)P is responsible for the recruitment of the Nox2 subunit p40^{phox}, which is integral to optimal production of NADPH oxidase and EEA-1, a tethering molecule that is essential for the progression of phagosome maturation.

Reference List

21. Basle,A., Rummel,G., Storici,P., Rosenbusch,J.P., & Schirmer,T. Crystal structure of osmoporin OmpC from E. coli at 2.0 A. *J Mol Biol*. **362**, 933-942 (2006).

Figure S1. Absence of major a developmental defect in *Slamf1*$^{-/-}$ macrophages.

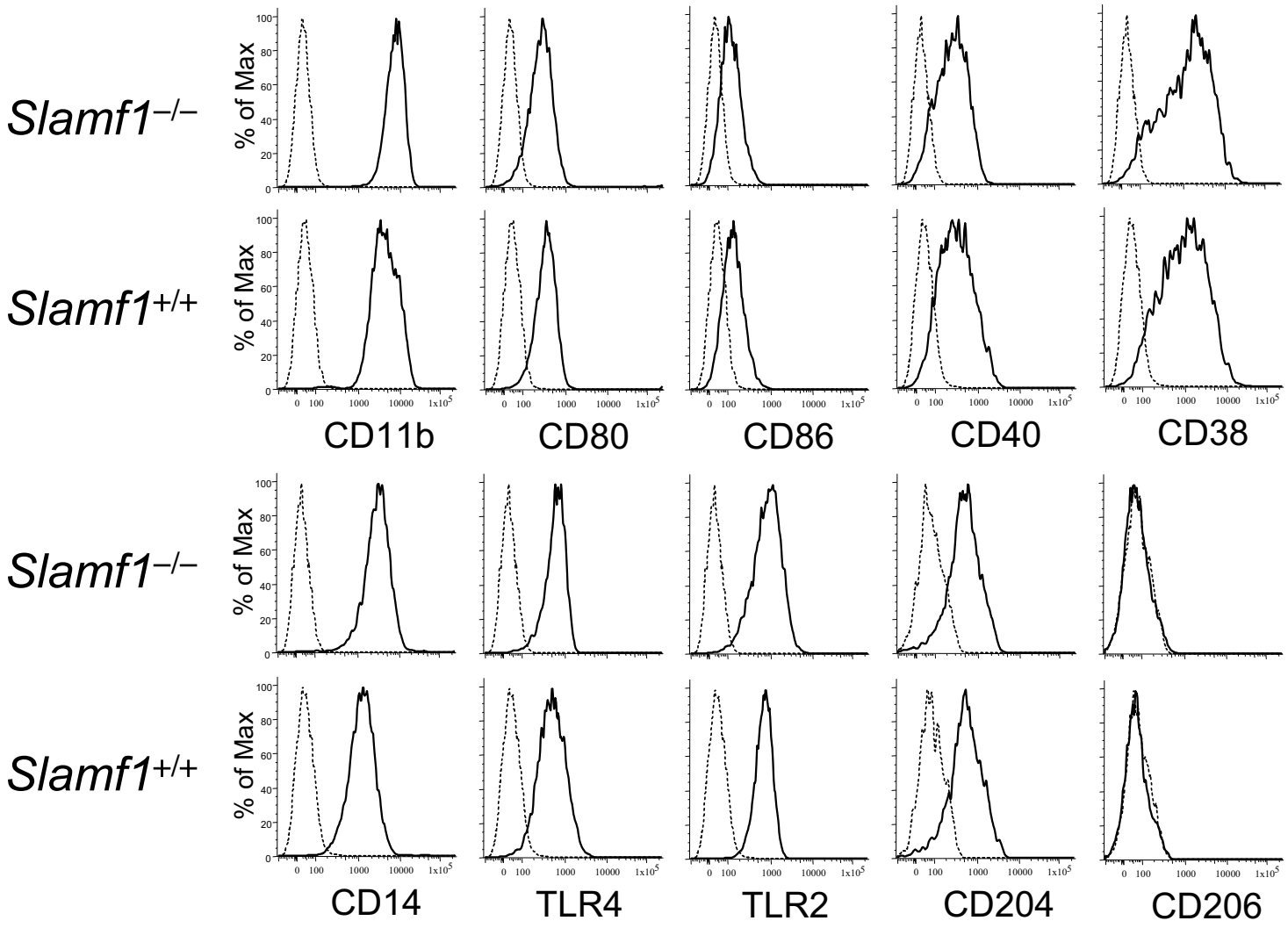

Nature Immunology: doi:10.1038/ni.1931

Figure S2. Defective killing of *E. coli* F18 by *Slamf1*$^{-/-}$ B6 primary peritoneal macrophages mice.

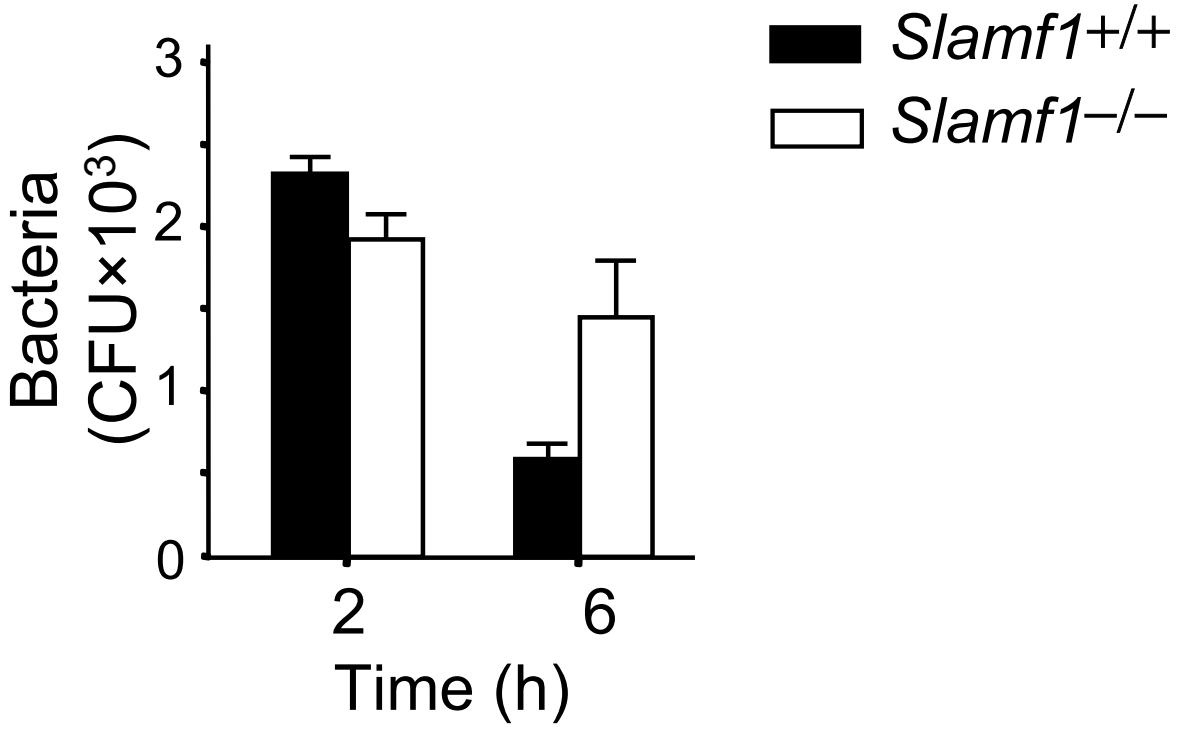

Nature Immunology: doi:10.1038/ni.1931

Figure S3. The *Slamf1*$^{-/-}$ B6 mice contain the 129 locus, as judged by cytofluorometric analyses of thymocytes and NK cells with haplotype specific antibodies directed against CD229 (129) and CD244 (B6).

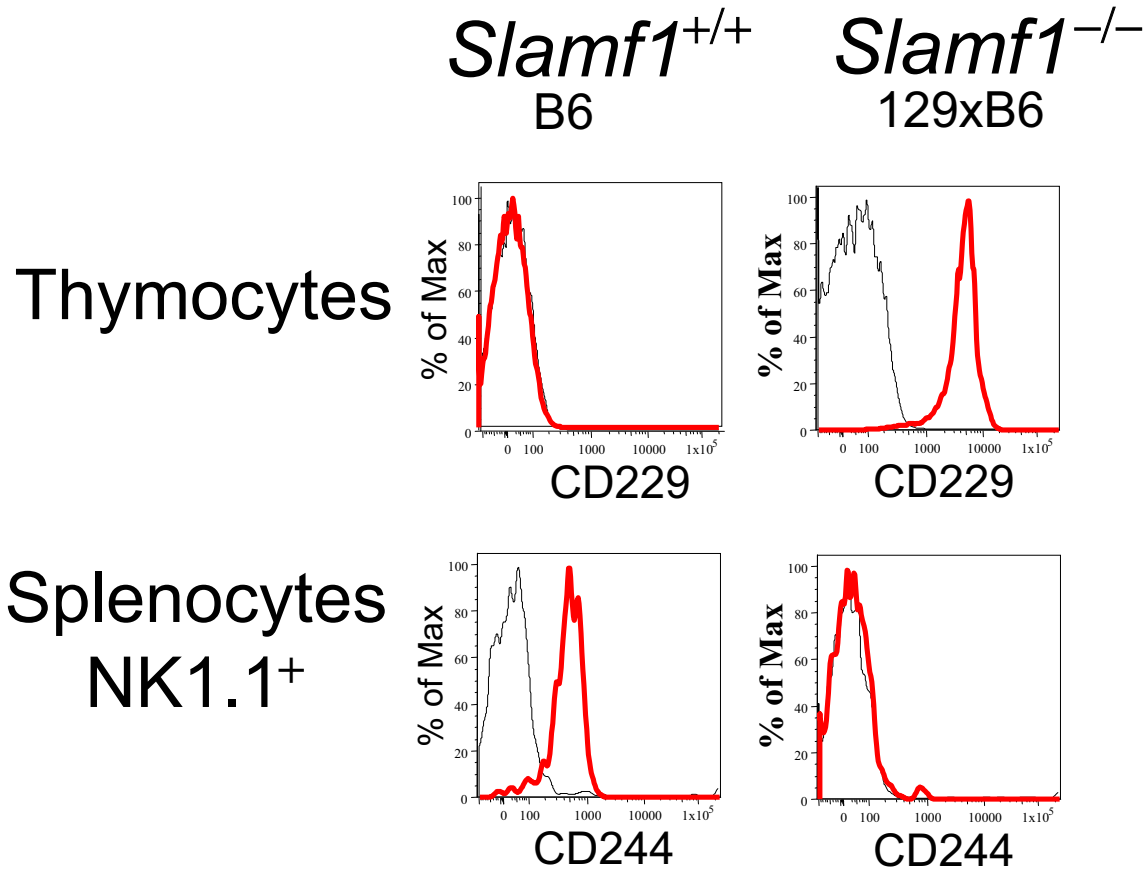

Nature Immunology: doi:10.1038/ni.1931

Figure S4. Both *Slamf1*$^{-/-}$ {129 x B6} and *Slamf1*$^{-/-}$ {129 x BALB/c} mice contain the 129 (SLAM - Family Haplotype II) derived SLAM-Family locus, as judged by RFLP.

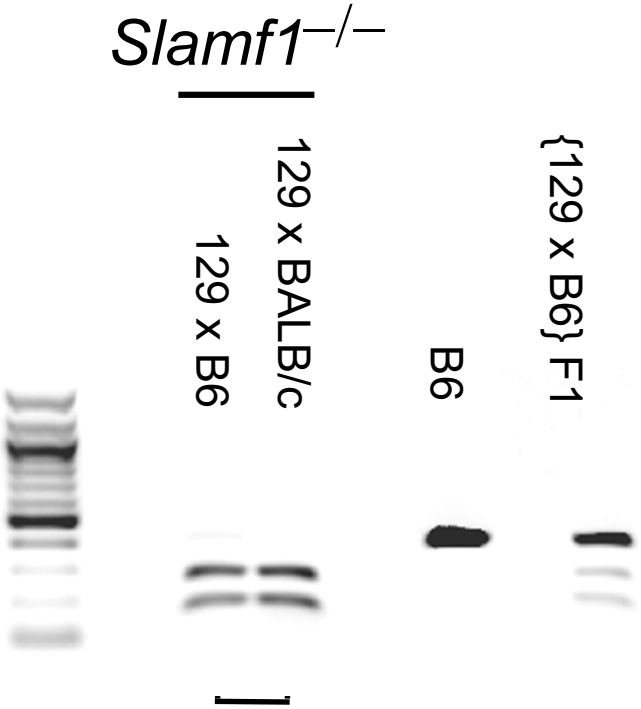

Nature Immunology: doi:10.1038/ni.1931

Figure S5. Defective Nox2 activity by *Slamf1*$^{-/-}$ B6 primary macrophages in response to *E.coli* F18.

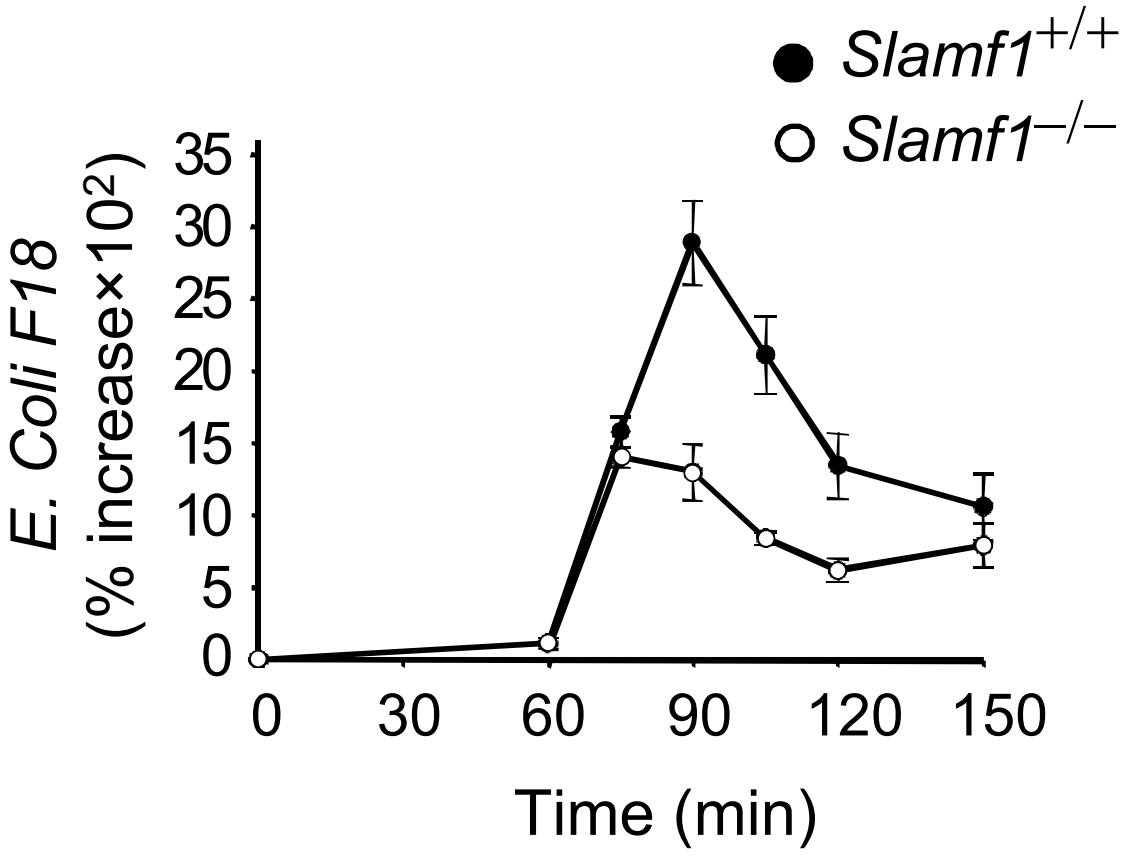

Nature Immunology: doi:10.1038/ni.1931

Figure S6. Increased Nox2 activity upon phagocytosis of *E.coli* F18 by *Slamf1*-transfected RAW 264.7 macrophages.

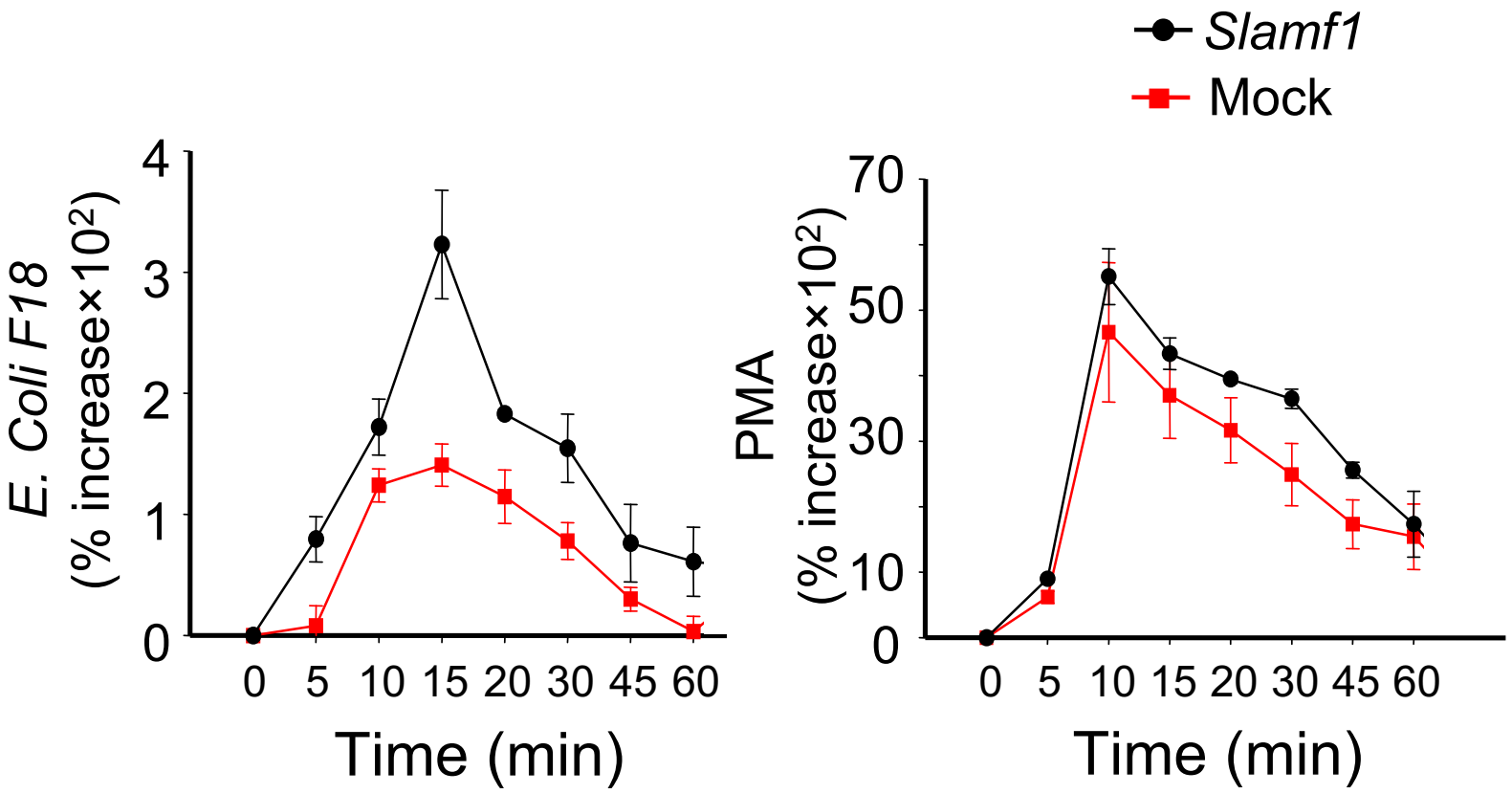

Nature Immunology: doi:10.1038/ni.1931

Figure S7. Transferrin- endocytosis is not altered in *Slamf1*-/- primary macrophages.

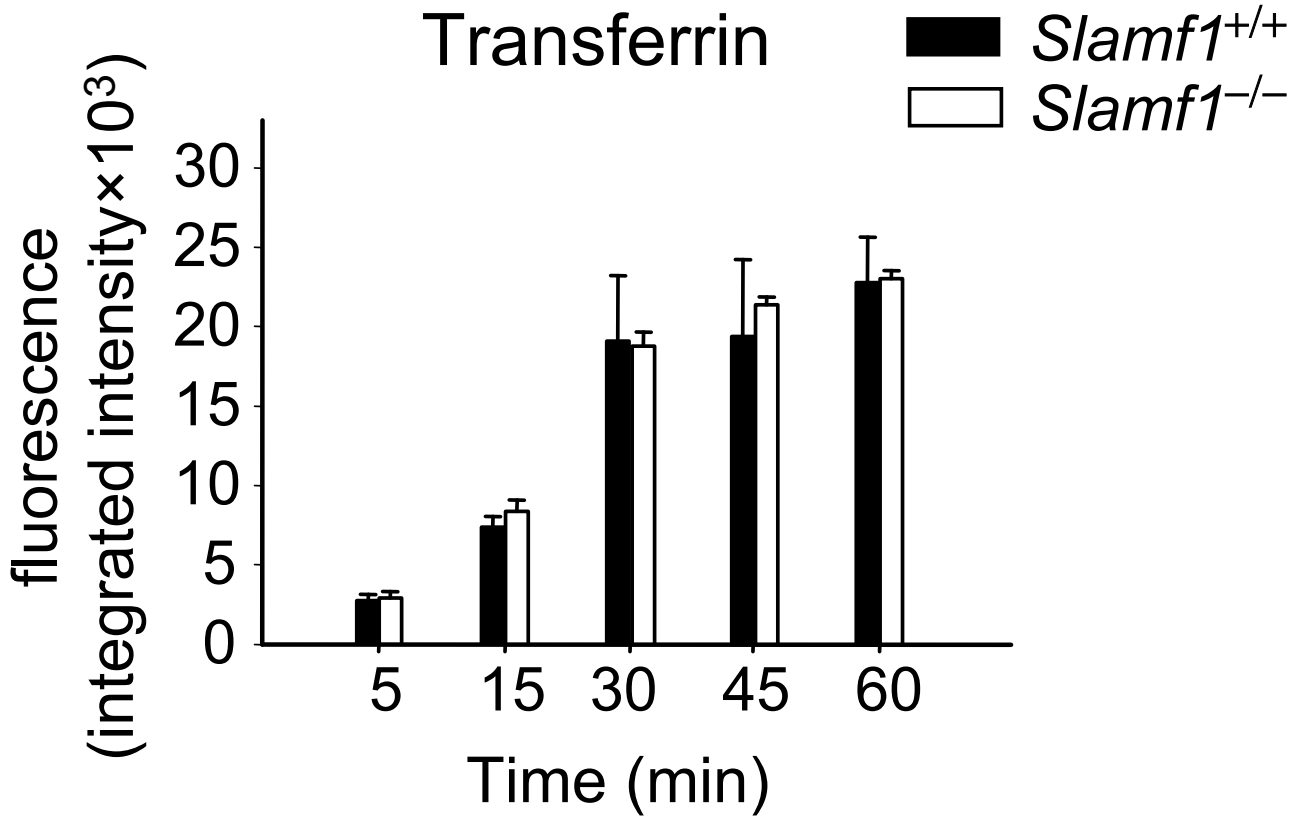

Nature Immunology: doi:10.1038/ni.1931

Figure S8. Low density lipoprotein (LDL) endocytosis is not altered in *Slamf1*-/- primary macrophages.

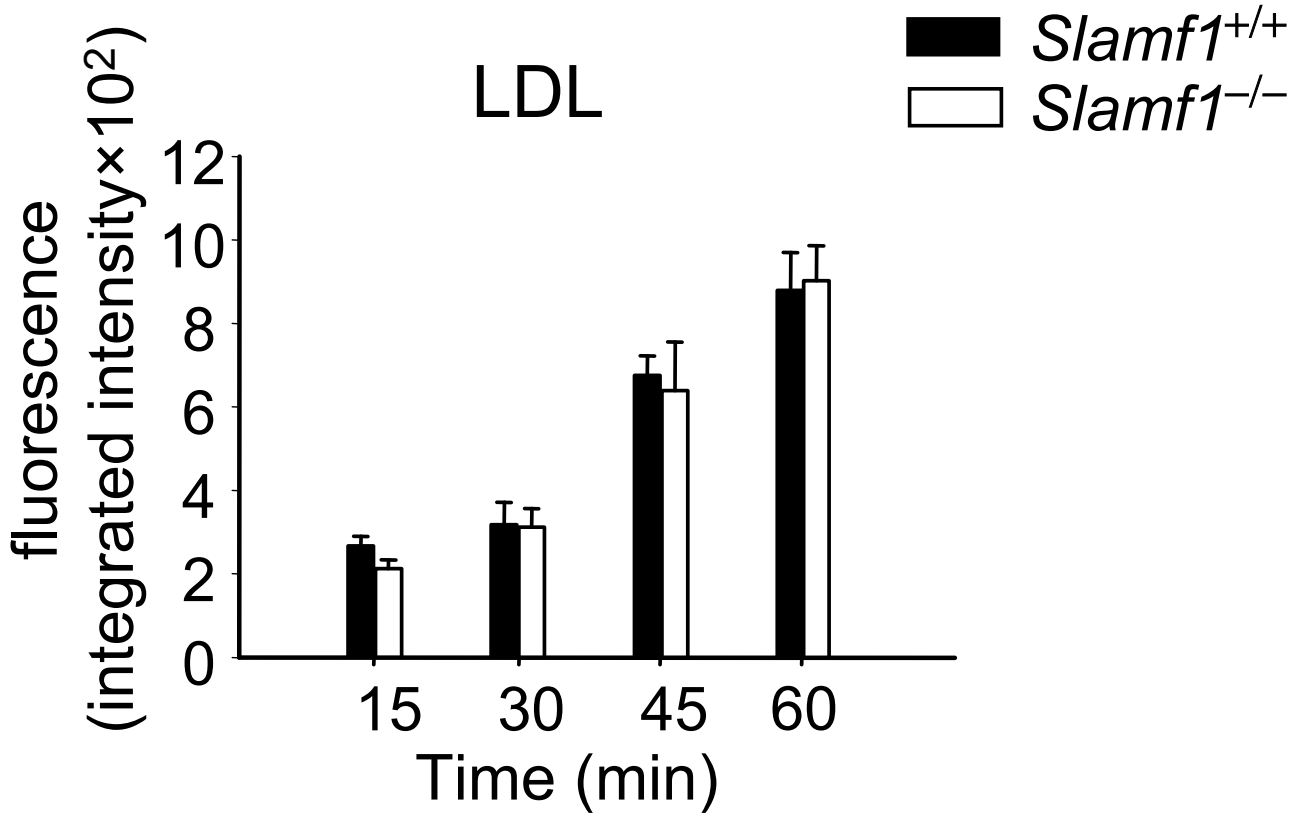

Nature Immunology: doi:10.1038/ni.1931

Figure S9. Delayed recruitment of Rab5 to crude extract-bead phagosomes of primary peritoneal macrophages isolated from *Slamf1*$^{-/-}$ BALB/c mice.

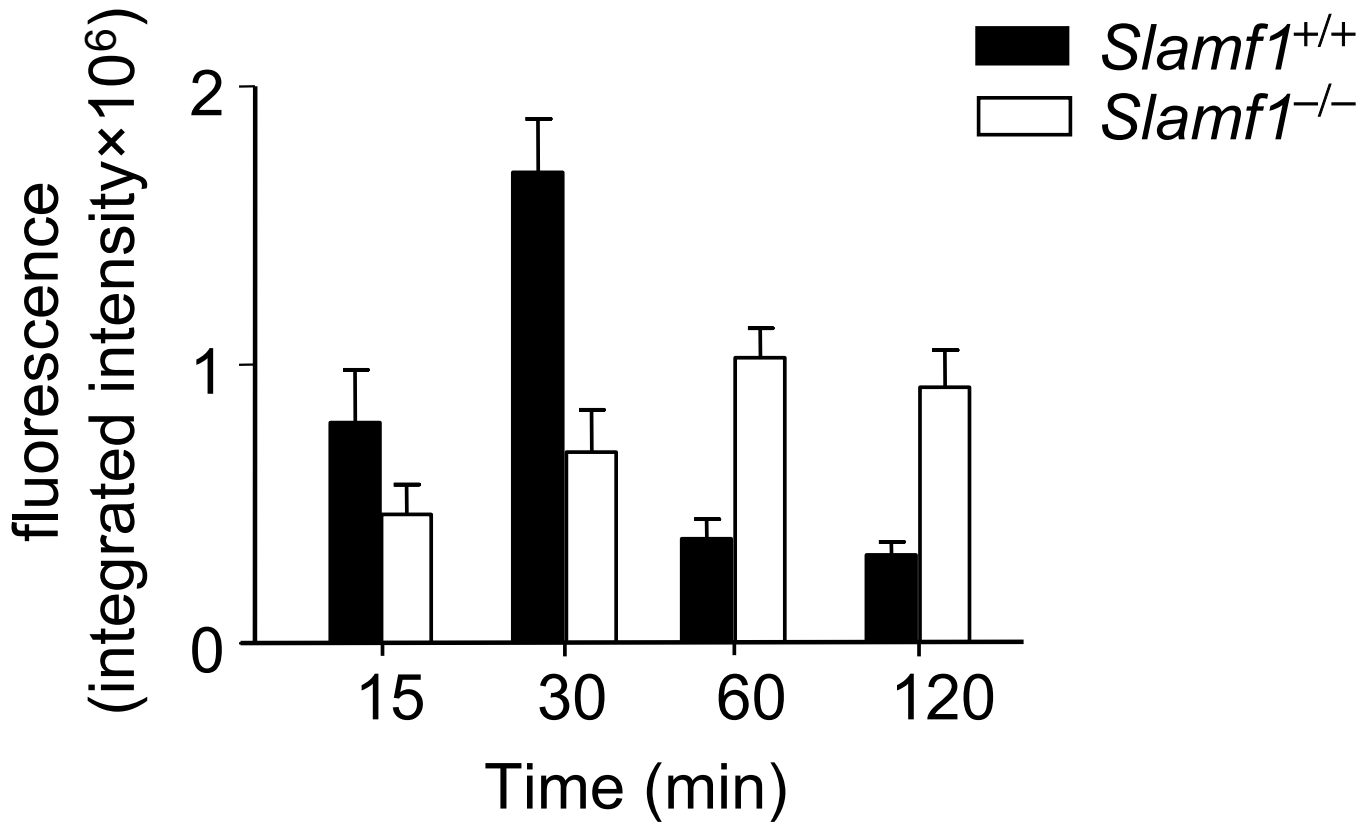

Nature Immunology: doi:10.1038/ni.1931

Figure S10. Western blot of ΔIgV-CD3ζ *Slamf1* expressed in Jurkat cells.

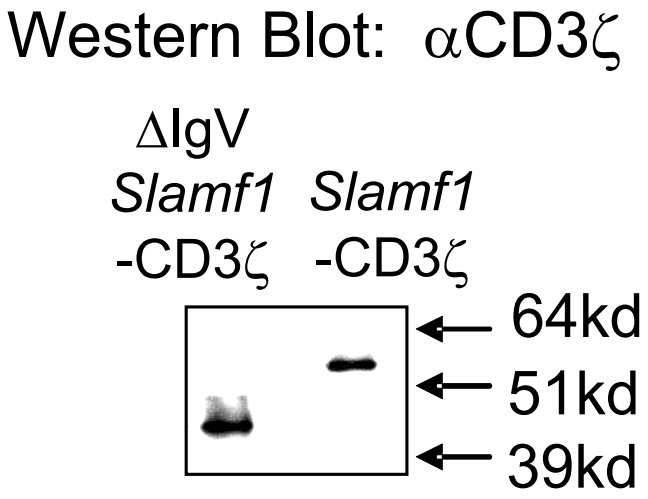

Nature Immunology: doi:10.1038/ni.1931

Figure S11. *Slamf1* recognizes various strains of *E. Coli*.

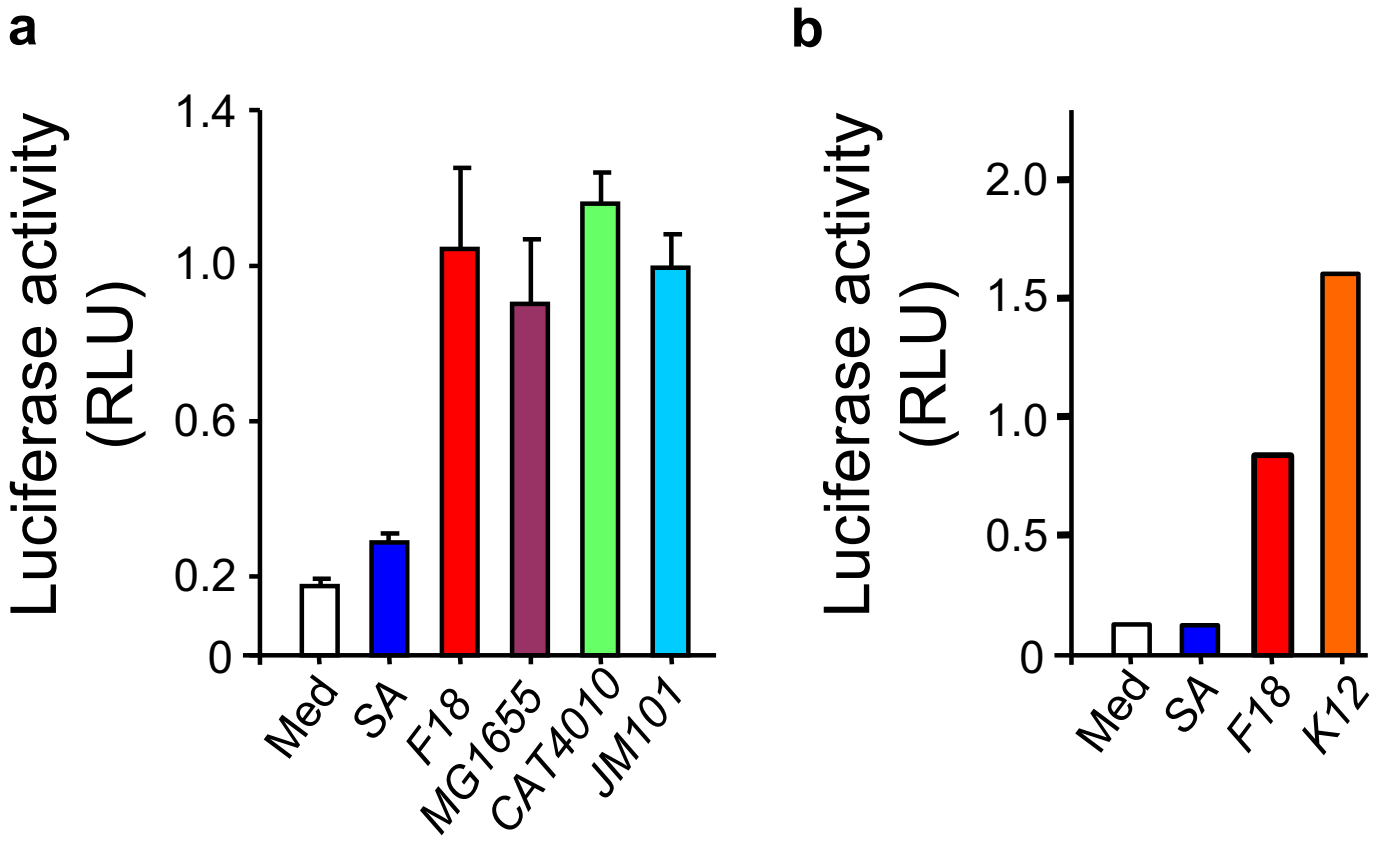

Nature Immunology: doi:10.1038/ni.1931

Figure S12. High degree of homology between the loop regions of OmpC and OmpF from *E. coli* and S. *typhimurium*.

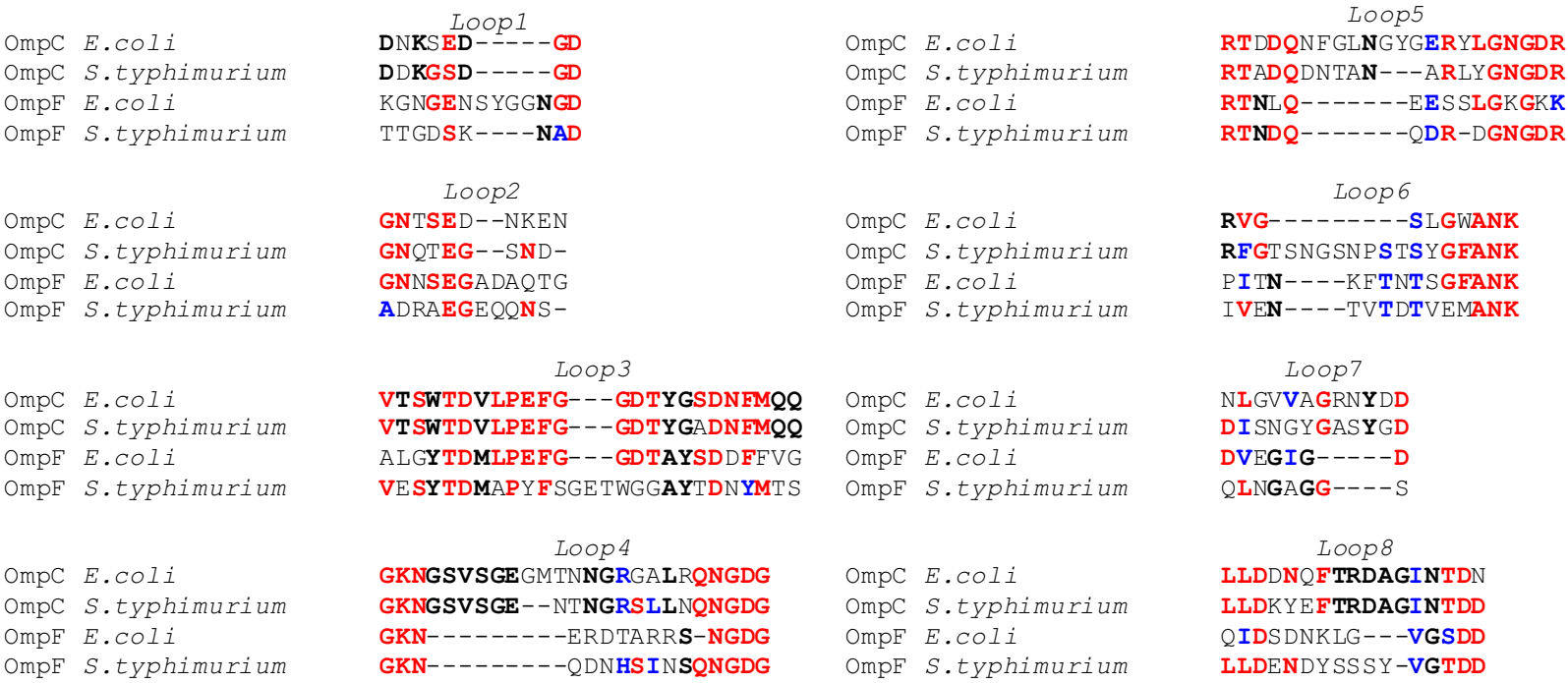

Nature Immunology: doi:10.1038/ni.1931

Figure S13. *Slamf1*-/- macrophages have no defect in Nox2 activity in response to an OmpC and OmpF double deficient *E. coli* mutant.

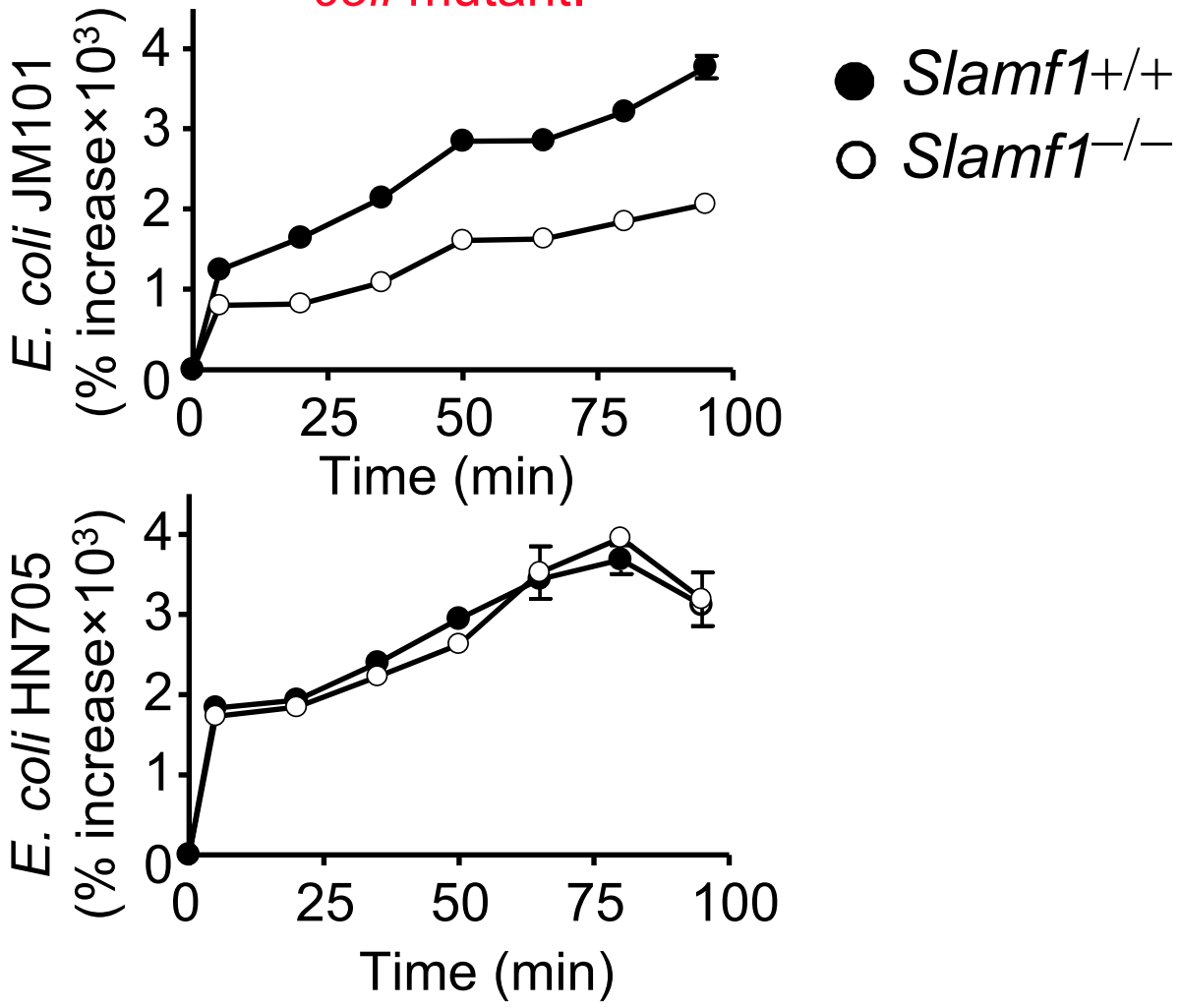

Nature Immunology: doi:10.1038/ni.1931

Figure S14. Model showing regulation of Gram-negative bacterial killing by SLAM.

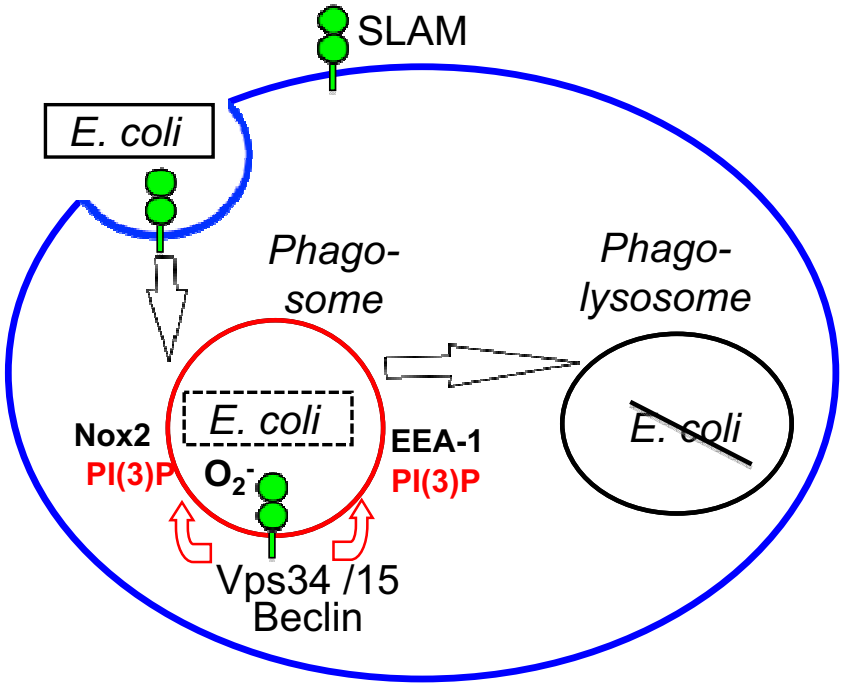

Nature Immunology: doi:10.1038/ni.1931